The Fusarium oxysporum Avr2-Six5 Effector Pair Alters Plasmodesmatal Exclusion Selectivity to Facilitate Cell-to-Cell Movement of Avr2

Cao, L.; Blekemolen, M.C.; Tintor, N.; Cornelissen, B.J.C.; Takken, F.L.W.

DOI
10.1016/j.molp.2018.02.011

Publication date
2018

Document Version
Final published version

Published in
Molecular Plant

Molecular Plant
Research Article

CellPress
PARTNER JOURNAL

The *Fusarium oxysporum* Avr2-Six5 Effector Pair Alters Plasmodesmatal Exclusion Selectivity to Facilitate Cell-to-Cell Movement of Avr2

Lingxue Cao, Mila C. Blekemolen, Nico Tintor, Ben J.C. Cornelissen and Frank L.W. Takken*

Molecular Plant Pathology, Swammerdam Institute for Life Science, University of Amsterdam, 1098 XH Amsterdam, the Netherlands

***Correspondence: Frank L.W. Takken (f.l.w.takken@uva.nl)**

https://doi.org/10.1016/j.molp.2018.02.011

ABSTRACT

Pathogens use effector proteins to manipulate their hosts. During infection of tomato, the fungus *Fusarium oxysporum* secretes the effectors Avr2 and Six5. Whereas Avr2 suffices to trigger *I-2*-mediated cell death in heterologous systems, both effectors are required for *I-2*-mediated disease resistance in tomato. How Six5 participates in triggering resistance is unknown. Using bimolecular fluorescence complementation assays we found that Avr2 and Six5 interact at plasmodesmata. Single-cell transformation revealed that a 2xRFP marker protein and Avr2-GFP only move to neighboring cells in the presence of Six5. Six5 alone does not alter plasmodesmatal transduction as 2xRFP was only translocated in the presence of both effectors. In *SIX5*-expressing transgenic plants, the distribution of virally expressed *Avr2-GFP*, and subsequent onset of *I-2*-mediated cell death, differed from that in wild-type tomato. Taken together, our data show that in the presence of Six5, Avr2 moves from cell to cell, which in susceptible plants contributes to virulence, but in *I-2* containing plants induces resistance.

Key words: Plasmodesmata, immunity, effector, pathogen, Fusarium, disease

Cao L., Blekemolen M.C., Tintor N., Cornelissen B.J.C., and Takken F.L.W. (2018). The *Fusarium oxysporum* Avr2-Six5 Effector Pair Alters Plasmodesmatal Exclusion Selectivity to Facilitate Cell-to-Cell Movement of Avr2. Mol. Plant. **11**, 691–705.

INTRODUCTION

Plants are challenged by a wide variety of pathogens such as bacteria, fungi, oomycetes, and nematodes. Plants have evolved a multi-layered immune system, by which they recognize and defend themselves against these biotic stresses (Jones and Dangl, 2006). Recognition of pathogen-associated molecular patterns (PAMPs) by dedicated plasma membrane-localized pattern recognition receptors results in PAMP-triggered immunity (PTI). To overcome PTI and facilitate infection, pathogens produce effector proteins. To counteract effector action, plants have developed a second layer of defense called effector-triggered immunity. The latter immune system relies on immune receptors, called resistance proteins, which specifically perceive effectors and subsequently mount immune responses.

Fusarium oxysporum is a root-infecting fungal pathogen causing wilt disease on a wide variety of plants (Michielse and Rep, 2009). Tomato is the only host of *F. oxysporum* f. sp. *lycopersici* (*Fol*). *Fol* invades roots and progresses through epidermal and endodermal tissues to eventually colonize the xylem vessels (Michielse and Rep, 2009). In the xylem sap of *Fol*-infected tomato, 14 *Fol*-derived small "Secreted-in-Xylem" (Six) proteins have been identified (Houterman et al., 2007; Schmidt et al., 2013). Among these, Six1, Six3, Six5, and Six6 have been shown to be required for *Fol* pathogenicity, defining them *sensu stricto* as effectors (Rep et al., 2004; Houterman et al., 2009; Gawehns et al., 2014; Ma et al., 2015). Besides contributing to virulence, some of these *Fol* effectors are recognized by tomato resistance (*R*) gene products, thereby conferring avirulence to the fungus. Three *Fol* Six proteins have been identified that trigger R protein-mediated resistances and these are renamed avirulence (Avr) proteins; Six1 (Avr3), Six3 (Avr2), and Six4 (Avr1) activate *I-3*-, *I-2*-, and *I-1*-mediated resistance, respectively (Takken and Rep, 2010).

Fol effectors Six3 (Avr2) and Six5 share a 1609-bp upstream promoter region that controls their expression (Schmidt et al., 2013). Together this pair of effectors is required to activate I-2-mediated immunity in tomato, and knockouts of each gene allows the fungus to overcome resistance (Ma et al., 2015). Although both genes are required for resistance, Avr2 alone suffices to trigger

Published by the Molecular Plant Shanghai Editorial Office in association with Cell Press, an imprint of Elsevier Inc., on behalf of CSPB and IPPE, SIBS, CAS.

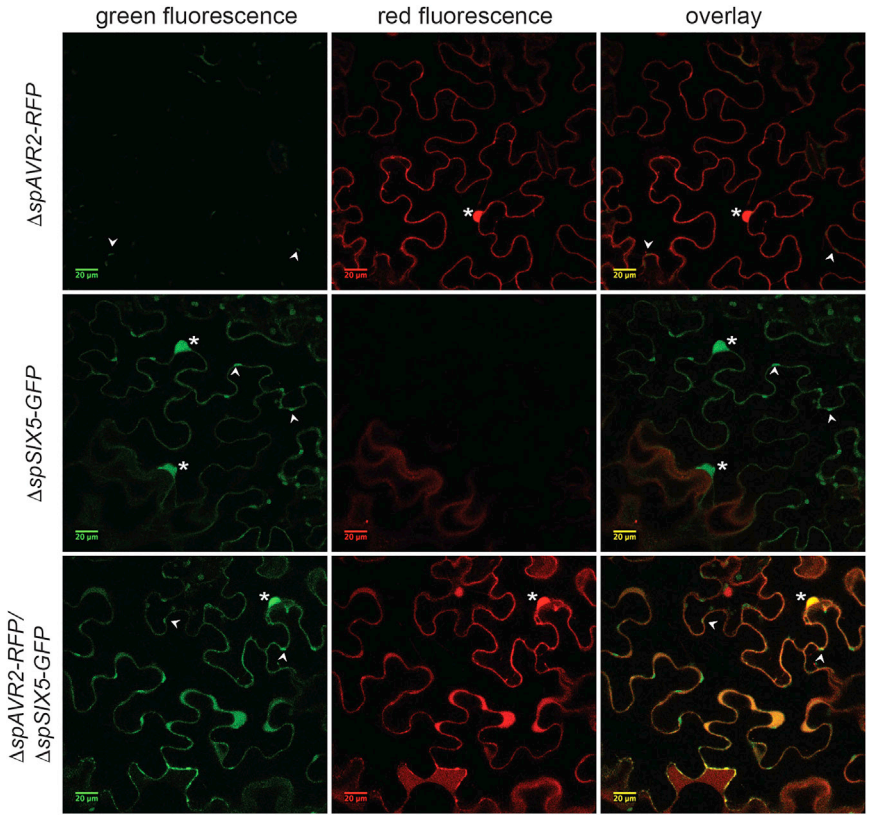

Figure 1. Avr2 and Six5 Co-localize in the Cytosol and Nucleus of Agro-Infiltrated *Nicotiana benthamiana* Cells.

ΔspAVR2-RFP, *ΔspSIX5-GFP*, or *ΔspAVR2-RFP*/*ΔspSIX5-GFP* were expressed in *N. benthamiana* leaves using agro-infiltration, and fluorescence was monitored using confocal microscopy. In *ΔspAVR2-RFP*-expressing *N. benthamiana* leaf epidermal cells, red fluorescence was observed in the cytosol and nucleus (labeled with asterisks). Green fluorescence, following *ΔspSIX5-GFP* agro-infiltration, was detected in both the cytosol and nucleus. Yellow fluorescence shows the co-localization of Avr2 and Six5 in the cytosol and nucleus following co-infiltration of *ΔspAVR2-RFP* and *ΔspSIX5-GFP*. Green fluorescent chloroplasts are marked by arrowheads.

I-2-mediated cell death when expressed in *Nicotiana benthamiana* or upon virus-based expression in *I-2* tomato (Houterman et al., 2009). *I-2* encodes a classical intracellular NB-LRR-type immune receptor (Simons et al., 1998). The resistance gene is specifically expressed in the parenchyma cells neighboring the xylem vessels (Mes et al., 2000). Although Avr2 has originally been identified in *Fol*-infected tomato xylem sap, the protein acts inside host cells where it suppresses PTI (Di et al., 2016, 2017). A nuclear localization of Avr2 is compulsory for recognition by I-2 (Ma et al., 2013). Previously it was shown that Avr2 interacts with Six5 in yeast-two-hybrid (Y2H) assays, as well as *in planta* following transient expression in *N. benthamiana* (Ma et al., 2015). Here, we investigate how Six5 contributes to Avr2 function and observed that Avr2 specifically interacts with Six5 at plasmodesmata. Together, the two effectors are shown to manipulate plasmodesmata and facilitate cell-to-cell movement of Avr2, but also of a 2xRFP marker protein. Our data suggest that Six5 contributes to the virulence of *Fol* by facilitating Avr2 movement via plasmodesmata. In a susceptible plant, this is beneficial to the pathogen. However, in a resistant plant, it will result in perception of Avr2 by the I-2 protein present in the xylem-adjacent cells, resulting in induction of immunity, and thereby halting the pathogen.

RESULTS

Avr2 and Six5 Interact at Plasmodesmata

The *Fol* effectors Avr2 and Six5 are required together to trigger I-2 protein-mediated resistance in tomato (Ma et al., 2015). To identify where in the cell these proteins exert their action(s), we examined the subcellular localization of Avr2 or Six5 alone as well as in combination using confocal microscopy. To visualize Avr2 and Six5, we made constructs encoding the two mature proteins (i.e., without their endogenous signal peptide [Δsp]) that were C-terminally fused to a red fluorescent protein (RFP) or a green fluorescent protein (GFP), respectively. Next, *ΔspAVR2-RFP* and *ΔspSIX5-GFP* were expressed in *N. benthamiana* leaves using *Agrobacterium*-mediated transformation. Similar to a previous report (Ma et al., 2013), red fluorescence was observed for *ΔspAVR2-RFP* in both the cytosol and the nucleus (Figure 1, upper panel, channels "red fluorescence" and "overlay"). In *N. benthamiana* epidermal cells, the cytosolic RFP signal can be seen as a diffuse signal at the cell periphery and in cytoplasmic strands, as the large vacuole confines the cytosol to a thin layer at the cell periphery. A similar pattern of nuclear and cytosolic green fluorescence was observed in cells expressing Six5-GFP (Figure 1, middle panel, channel "green fluorescence"), indicating an identical subcellular localization for Avr2-RFP and Six5-GFP. Chloroplasts of *N. benthamiana* epidermal leaf cells showed green autofluorescence (Figure 1, green fluorescence channel labeled with arrowheads) following *ΔspSIX5-GFP* and *ΔspAVR2-RFP* expression (Figure 1, arrowheads). To test whether accumulation of Avr2-RFP affects the subcellular localization of Six5-GFP, or vice versa, we co-expressed both constructs in *N. benthamiana* leaves (Figure 1, lower panel). The yellow color indicated the overlap of the green and red fluorescent signals produced by Avr2-RFP and Six5-GFP in the cytosol and nucleus of double transformed cells (Figure 1, lower panel, channel "overlay"). No apparent change in localization of either protein was observed when both proteins were co-expressed. Fusion of the fluorescent RFP or GFP proteins to the N terminus of either effector did not change their localization pattern, showing that the position of the tag does not affect the subcellular localization of the effectors (Supplemental Figure 1).

To further investigate the subcellular co-localization of Avr2 and Six5 and to localize a possible interaction between

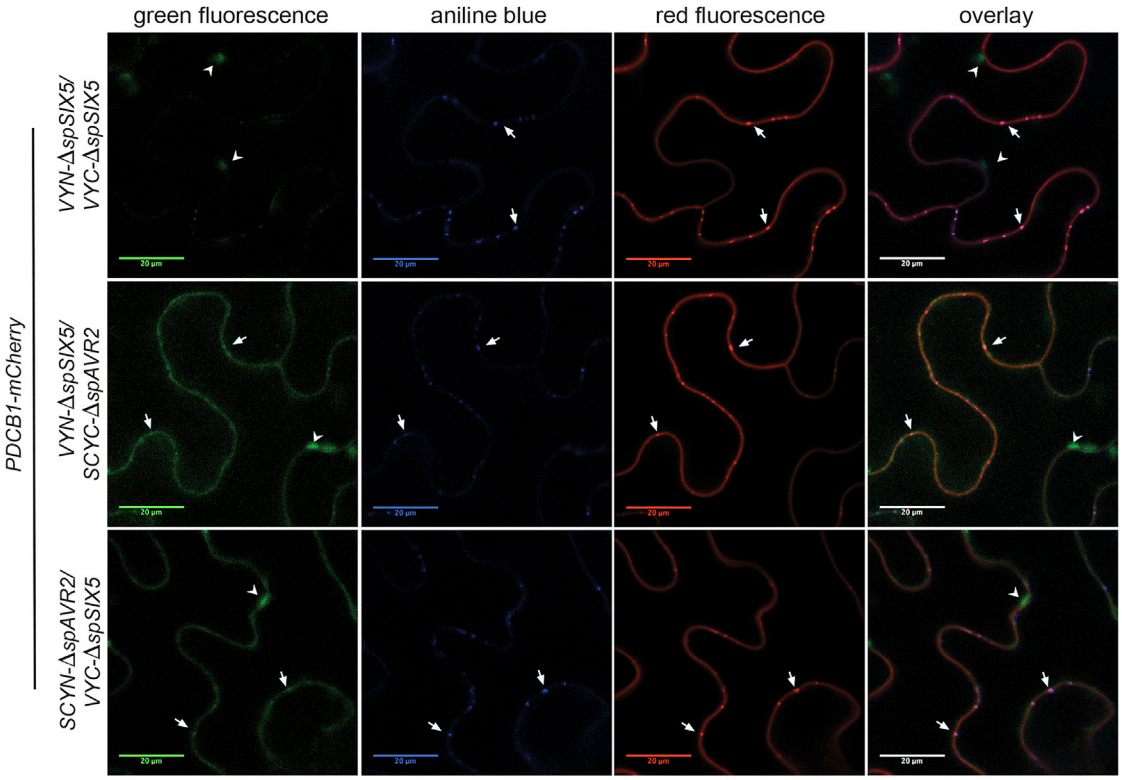

Figure 2. Avr2 and Six5 Co-localize and Interact at Plasmodesmata.

Confocal images of *N. benthamiana* leaves agro-infiltrated with BiFC constructs of VYN::*ΔspSIX5*, VYC::*ΔspSIX5*, SCYN::*ΔspAVR2*, and SCYC::*ΔspAVR2* (co-expressed with a plasmodesmatal marker protein, *PDCB1-mCherry*). No green fluorescence complementation was observed following co-expression of VYN::*ΔspSIX5* and VYC::*ΔspSIX5* (upper panel). Green fluorescence resulting from the interaction of VYN-ΔspSix5 and SCYC-ΔspAvr2 was observed in the cytosol and at spots (arrows) at the cell periphery (middle panel). The green spots co-localize with aniline blue-stained plasmodesmata-associated callose and with the red fluorescent signal emitted by m-Cherry-labeled PDCB1. Green fluorescence was also observed in the cytosol and at distinct spots at the cell periphery following expression of the reciprocally tagged *SCYN-ΔspAVR2* and *VYC-ΔspSIX5* combination (bottom panel). Aniline blue-stained plasmodesmata-associated callose and the red fluorescent plasmodesmata labeled by PDCB1-mCherry both co-localize with these green fluorescent spots. Green autofluorescent chloroplasts are marked by arrowheads.

these two proteins, we performed bimolecular fluorescence complementation (BiFC) assays. To this end, Avr2 and Six5 were N-terminally tagged with either the N- or C-terminal half of yellow fluorescent protein (YFP) variants (Gehl et al., 2009). A very close proximity of, or an interaction between, two proteins that are each tagged with the opposite half of the fluorescent protein results in the ability to fluoresce upon excitation of the complemented fluorophore. To assess a potential interaction, we transiently produced both effectors in *N. benthamiana* epidermal leaf cells and monitored fluorescence by confocal microscopy. The following constructs were used: *VYN*::*ΔspSIX5* (encoding the N-terminal half of Venus YFP [VY] tagged to Six5), *VYC*::*ΔspSIX5* (Six5 with the C-terminal half of VY), *SCYN*::*ΔspAVR2* (Avr2 with the N-terminal half of SCY), and *SCYC*::*ΔspAVR2*. The *AVR2* and/or *SIX5* constructs were also co-expressed with a construct encoding RFP (mCherry) labeled plasmodesmata-marker protein PDCB1 (plasmodesmata callose-binding protein 1, see below). Green fluorescence is indicative of a Six5–Avr2 interaction due to complementation of the YFP/CFP halves. Upon co-expression of *VYN*::*ΔspSIX5* and *VYC*::*ΔspSIX5*, no green fluorescence was observed except for autofluorescent chloroplasts (Figure 2, upper panel, arrowheads). This result implies that, in contrast to Avr2, which forms homo-dimers in *N. benthamiana* cells, Six5 does not homo-dimerize *in planta* and hence may serve as a negative control for the assay (Ma et al., 2015). Upon co-expression of *VYN*::*ΔspSIX5* and *SCYC*::*ΔspAVR2* (Figure 2, middle panel; Supplemental Figure 2), green fluorescence was observed in the cytosol (but not the nucleus) and in spots at the cell periphery (indicated by arrows). The same pattern was observed for the reverse situation when *SCYN*::*ΔspAVR2* and *VYC*::*ΔspSIX5* were co-expressed (Figure 2, lower panel). These spots were not observed upon co-expression of *ΔspAVR2-RFP* and *ΔspSIX5-GFP* (Figure 1), which might imply that only a minority of the effectors interact at these spots and that the larger cytoplasmic pool overshadows the fluorescence signal. The BiFC signal strongly suggests an interaction between Avr2 and Six5 *in planta* at two distinct subcellular locations: the aforementioned spots and the cytoplasm.

To reveal the identity of the fluorescent Avr2/Six5 spots, we determined their dynamics and mobility using time-lapse imaging over a 30-min interval (data not shown). The observed immobility of the fluorescent spots in combination with their localization at the cell periphery suggests that Avr2 and Six5 are interacting at a structure that is tethered to the cell wall. Given their localization and immobile character, we therefore examined whether the dots co-localize with plasmodesmata, a plant cell structure that fits

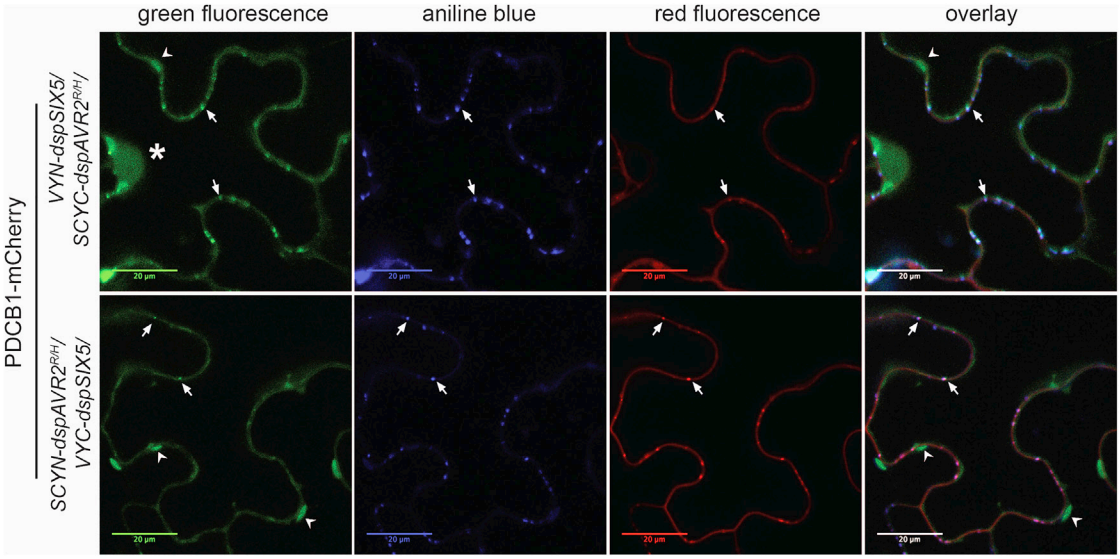

Figure 3. The *I-2* Breaking Avr2$^{R/H}$ Variant Interacts with Six5 at Plasmodesmata.
VYN-ΔspSix5/SCYC-ΔspAvr2$^{R/H}$ or *SCYN-ΔspAvr2$^{R/H}$/VYC-ΔspSix5* were agro-infiltrated together with *PDCB1-mCherry* in *N. benthamiana* leaves and visualized using confocal microscopy. Green fluorescence produced by complementation of the *VYN-ΔspSix5/SCYC-ΔspAvr2$^{R/H}$* BiFC pair was observed in the cytosol and at spots (arrows) at the cell periphery. Occasionally, green fluorescence was found in the nucleus (marked with an asterisk next to the nuclei). Green fluorescence was also observed in the cytosol and at spots at the cell periphery following co-infiltration of the reciprocal *SCYN-ΔspAvr2$^{R/H}$/VYC-ΔspSix5* combination. The green fluorescent spots co-localize with both aniline blue-stained plasmodesmatal callose and with the red PDCB1-mCherry. Green fluorescent chloroplasts are marked by arrowheads.

such characteristics. To this end, plasmodesmata-associated callose was stained with aniline blue in *N. benthamiana* leaves that co-express the *ΔspAVR2/ΔspSIX5* BiFC pair (Figure 2, aniline blue channel of the middle and lower panels). The Avr2/Six5 BiFC dots perfectly overlapped with aniline blue-stained callose (Figure 2, overlay channel of the middle and lower panels), suggesting that the Avr2/Six5 interaction indeed occurs at plasmodesmata. To further substantiate this finding, we co-expressed the gene encoding the plasmodesmatal marker protein PDCB1-mCherry with the *ΔspAVR2/ΔspSIX5* BiFC constructs. Overexpression of PDCB1-mCherry resulted in bright red fluorescence at plasmodesmata and a weak background signal that might originate from ER-resident PDCB1-mCherry, (Figure 2, red fluorescence channel). The red fluorescent spots originating from PDCB1-mCherry overlapped with the green fluorescence signals originating from the Avr2/Six5 interaction and with the blue fluorescence of the aniline blue-stained callose (Figure 2, overlay). Furthermore, in the absence of an aniline blue stain, the red PDCB1-mCherry and the green Avr2/Six5 BiFC fluorescence overlapped, showing that the apparent co-localization was not an artifact induced by the staining procedure (data not shown). Taken together, Avr2-RFP and Six5-GFP were observed to accumulate in both the cytosol and nucleus. However, an interaction was only observed in the cytosol and at specific spots co-localizing with plasmodesmata.

An I-2 Breaking Avr2 Variant Also Interacts with Six5 at Plasmodesmata

Single amino acid substitutions in Avr2 enable *Fol* race 3 isolates to evade I-2 recognition and to cause disease on *I-2* containing plants (Houterman et al., 2009). To investigate whether escape of I-2 recognition is related to an altered interaction (pattern) of the Avr2 variant with Six5, we compared the co-localization of both proteins *in planta* with the localization of wild-type Avr2 and Six5. The Avr2$^{R/H}$ variant, harboring amino acid substitution R45H, was tagged at its N terminus with either SCYN or SCYC. The constructs were co-expressed with either *VYC-ΔspSIX5* or *VYN-ΔspSIX5* in *N. benthamiana* leaves by agro-infiltration. Green fluorescence was observed from both the VYN-ΔspSix5/SCYC-ΔspAvr2$^{R/H}$ and the SCYN-ΔspAvr2$^{R/H}$/VYC-ΔspSix5 combinations, thus indicating an interaction between both proteins *in planta* (Figure 3, green fluorescence channel). Similar to the interaction of the Avr2/Six5 pair, green fluorescence was observed in the cytosol and in spots at the cell periphery; occasionally, a weak GFP signal was also detected in the nucleus following *ΔspAVR2$^{R/H}$/ΔspSIX5* expression (Figure 3). Similar to wild-type Avr2, the spots at the cell periphery co-localized with plasmodesmata, as shown by both staining of plasmodesmatal callose and co-expression with PDCB1-mCherry (Figure 3, overlay). These results show that the Avr2 variant from a *Fol* race 3 isolate interacts with Six5 when produced in *N. benthamiana* leaves, implying that the inability of I-2 to recognize Avr2$^{R/H}$ is not linked to an altered interaction pattern of Avr2 with Six5.

Six5 and Avr2 Facilitate Protein Transport through Plasmodesmata

Since the interaction between Avr2 and Six5 was observed at plasmodesmata, we speculated that *Fol* infection might involve manipulation of plasmodesmata, possibly, to facilitate effector transport and/or performance. Although both Avr2 and Six5 are required to trigger I-2 protein-mediated resistance, Avr2 alone is sufficient to initiate I-2 protein-mediated hypersensitive response (HR) in *N. benthamiana* (Ma et al., 2015). This discrepancy may be explained by the assumption that during natural infection of tomato, *Fol*-produced Six5 is required to

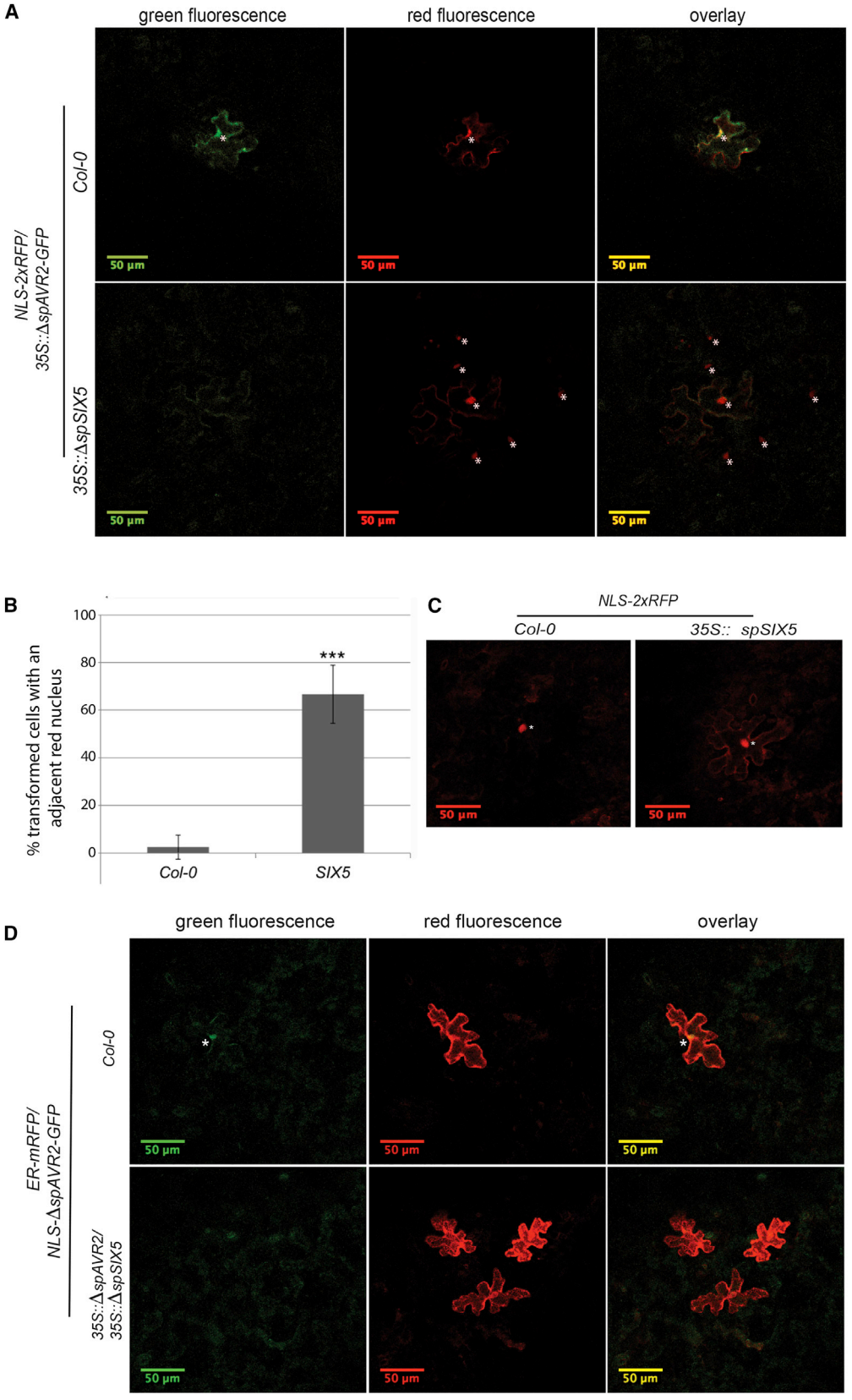

(legend on next page)

facilitate symplastic translocation of Avr2 to I-2-containing cells. As shown previously, *I-2* is highly expressed in the vasculature tissues in which resistance to the fungus is exerted (Mes et al., 2000). Cell-to-cell movement of Avr2 from cortical cells to *I-2*-expressing xylem parenchyma cells would allow the plant to perceive the pathogen and mount its defenses, while in the absence of Six5 the plant is blind to the presence of the effector protein. To test this hypothesis and determine whether the presence of Six5 alters the cellular mobility of Avr2, we performed single-cell transformation experiments. Single-cell transformations were performed in wild-type *Arabidopsis thaliana* and in a transgenic line that constitutively expresses *ΔspSIX5* driven by the CaMV 35S promoter (see Methods). Four-week-old wild-type (*Col-0*) and *35S*::*ΔspSIX5 A. thaliana* leaves were bombarded with gold particles coated with a *ΔspAVR2-GFP* construct. To facilitate identification of transformed cells, we co-delivered a marker construct encoding a nuclear localization signal (NLS)-tagged double RFP (NLS-2xRFP). The molecular mass of the NLS-2xRFP protein exceeds the size-exclusion limit (SEL) of plasmodesmata, thus its size will prevent movement of the protein into neighboring cells (Crawford and Zambryski, 2000). Twelve hours after particle bombardment, individual transformed *Col-0* cells were identified by the red fluorescence, which was detected predominantly in the nucleus (Figure 4A). Although some red fluorescence was also observed in the cytosol. These observations confirm the functionality of the NLS and show that NLS-2xRFP does not move to neighboring cells in wild-type *Col-0*. The cells transformed with *ΔspAVR2-GFP* showed green fluorescence in the cytosol and nucleus which resembled the expression pattern observed in *N. benthamiana* (Figure 1A and Supplemental Figure 1). Whereas a bright green fluorescence was observed in bombarded *Col-0* leaves, only a very weak green fluorescence was apparent in the transformed cells of bombarded *35S*::*ΔspSIX5* leaves (Figure 4A). This observation may be explained by the assumption that Avr2-GFP is readily transported through plasmodesmata in the presence of Six5, resulting in a weak signal in the primary transformed cells. Consistent with this idea, we observed that red fluorescence originating from the NLS-2xRFP marker protein was often observed in the nuclei of cells neighboring the primary transformed cell in bombarded *ΔspSIX5*-transgenic leaves (Figure 4A, red fluorescence channel). Appearance of red fluorescence in neighboring cells implies cell-to-cell movement of the 2xRFP marker protein to adjacent cells. To quantify the extent of 2xRFP translocation in *ΔspSIX5* plants, we counted the number of single cells and clusters of cells showing red nuclei. Following particle bombardment of *35S*::*ΔspSIX5 A. thaliana* leaves, over 65% of the transformed (i.e., *NLS-2xRFP* expressing) cells showed a nuclear-localized RFP signal in at least one of their adjacent cells (Figure 4B). In contrast, about 3% of the transformed cells in wild-type *A. thaliana* showed red fluorescence in nuclei of cells neighboring the transformed cells. Therefore, in the presence of Six5 and Avr2, the NLS-2xRFP marker efficiently translocates to adjacent cells, implying that the SEL of plasmodesmata for this chimeric protein was modified in the presence of both effector proteins.

To examine whether Six5 alone suffices for the symplastic movement of NLS-2xRFP, we carried out single-cell transformations with *NLS-2xRFP* in wild-type and *ΔspSIX5*-expressing *A. thaliana.* In both plant lines, red fluorescence emitted by NLS-2xRFP was observed only in nuclei of individual transformed cells, but not in neighboring cells (Figure 4C). This suggests that intercellular translocation of NLS-2xRFP through plasmodesmata requires the presence of both Six5 and Avr2.

Six5 Mediates Intercellular Translocation of Avr2 in *A. thaliana* and *N. benthamiana*

The weak green fluorescence in cells expressing *ΔspAVR2-GFP* in the presence of Six5 (Figure 4A) suggests the transfer of the effector protein to neighboring cells and a concomitant reduction in amount of the protein in the transformed cell. No GFP signal was observed in neighboring cells, which might be due to the relatively low effector concentration distributed from merely a single transformed cell to all neighboring cells. To facilitate our detection of the protein in the neighboring cells, we fused Avr2 to an NLS and a GFP tag (*NLS-ΔspAVR2-GFP*) to concentrate the protein in the cell nucleus. The construct was expressed in *A. thaliana* leaves by particle bombardment. As a control for the transformation, a construct encoding a monomeric RFP (mRFP) with an HDEL ER retention signal (*ER-mRFP*) was co-bombarded with the *ΔspAVR2* construct. Confocal microscopy was performed 12 h after particle bombardment of *Col-0* and *35S*::*ΔspAVR2*/*35S*::*ΔspSIX5* transgenic *A. thaliana*. A *ΔspAVR2*/*ΔspSIX5* double transgenic *A. thaliana* line was

Figure 4. Avr2 and Six5 Are Both Required to Facilitate Intercellular Translocation of NLS-2xRFP in *Arabidopsis*.

(A) *ΔspAVR2-GFP* and *NLS-2xRFP*-carrying plasmids were co-bombarded into either *Col-0* or *35S*::*ΔspSIX5 Arabidopsis* leaves. Expression was monitored 12 h after bombardment using confocal microscopy. In *Col-0*, bright green fluorescence (Avr2-GFP) was observed in both the cytoplasm and nucleus of transformed cells. Only the nuclei (marked with asterisks) of these transformed cells showed red fluorescence (NLS-2xRFP). In transformed *35S*::*ΔspSIX5 Arabidopsis* cells, only very weak cytosolic green fluorescence was observed; red fluorescence was observed in both the nuclei of primary transformed cells and in their neighboring cells.

(B) The percentage of individual *ΔspAVR2-GFP* and *NLS-2xRFP* transformed cells in which NLS-2xRFP was present in neighboring cells of both wild-type and *35S*::*ΔspSix5 Arabidopsis*. For ±65% of the *35S*::*ΔspSix5 Arabidopsis* cells, NLS-2xRFP was observed to be translocated from the primary transformed cell to at least one adjacent cell. In *Col-0*, the percentage is approximately 3%. About 100 cells from five independent biological replicates were monitored. ***$p < 0.001$.

(C) Six5 alone is not sufficient to facilitate intercellular transport of NLS-2xRFP. An *NLS-2xRFP*-carrying plasmid was bombarded into either *Col-0* (left) or *35S*::*ΔspSIX5* (right) *Arabidopsis*. Red fluorescence was only observed in the nucleus (marked with an asterisk) of primary transformed cells for both wild-type and *ΔspSIX5 Arabidopsis*.

(D) *ER-mRFP* and *NLS-ΔspAVR2-GFP* constructs were co-bombarded into *Col-0* and *35S*::*ΔspAVR2*/*35S*::*ΔspSIX5 Arabidopsis*. The image shows ER-mRFP (red) and NLS-ΔspAvr2-GFP (green) in *Col-0* and in *35S*::*ΔspAVR2*/*35S*::*ΔspSIX5*. Note that the endoplasmic reticulum (ER) was labeled red by ER-mRFP in both lines; the green fluorescence of NLS-ΔspAvr2-GFP was readily observed in the nuclei (marked with a asterisk) of wild-type *Arabidopsis* cells, whereas it was rarely detected in *35S*::*ΔspAVR2*/*35S*::*ΔspSIX5* cells.

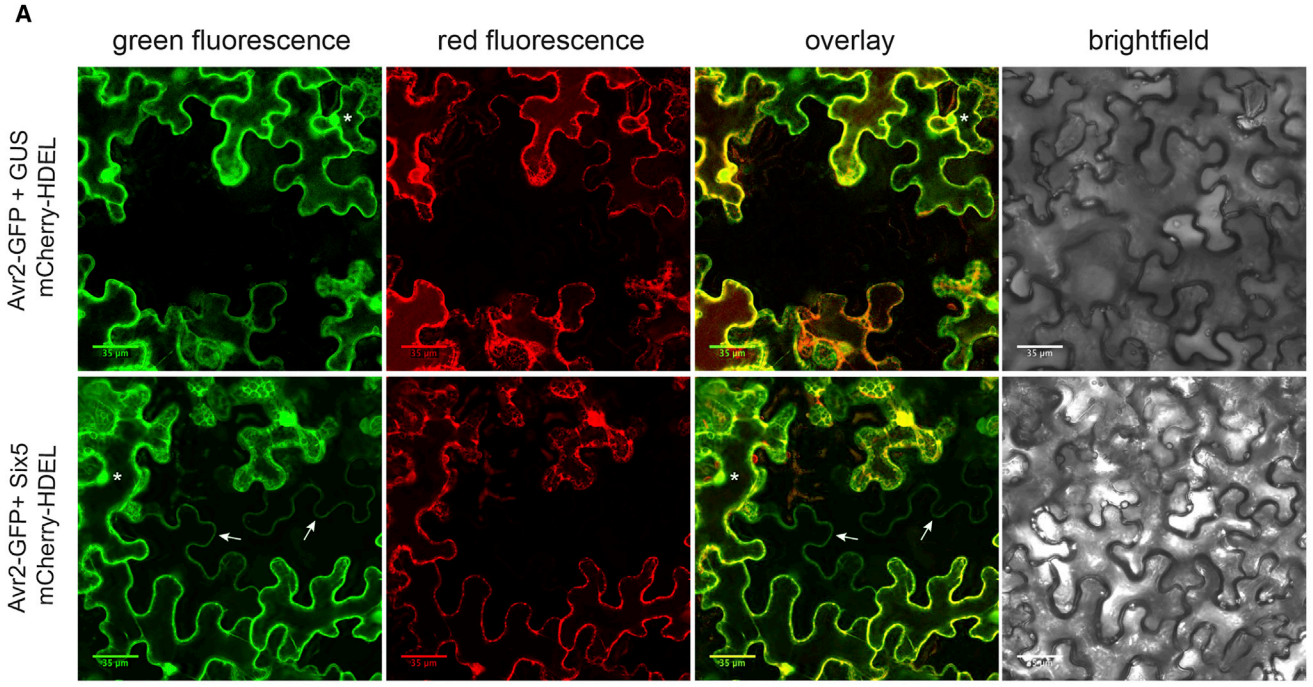

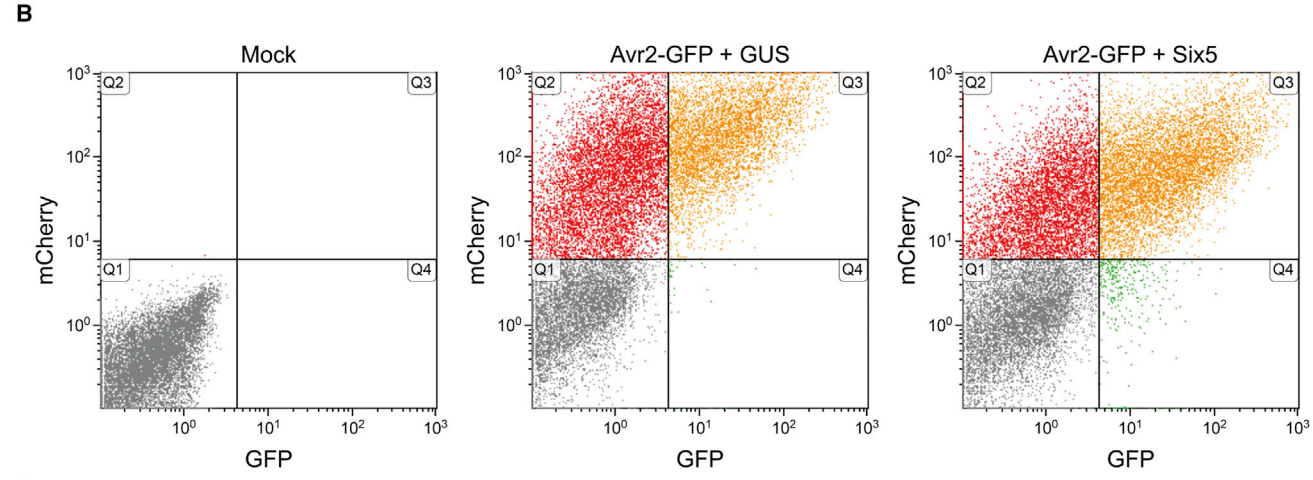

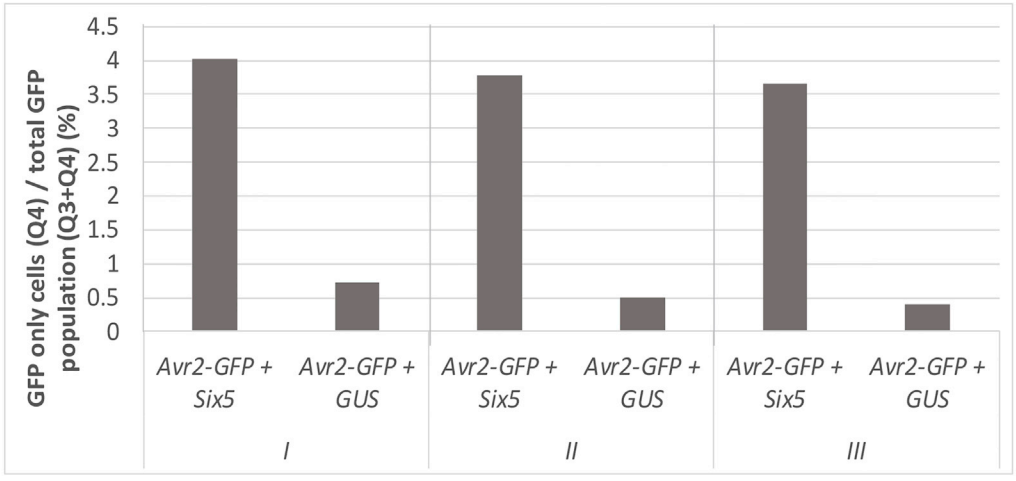

(legend on next page)

used to ensure sufficient amounts of mobile Avr2 and Six5 to interact and modulate the plasmodesmata. As expected, in *Col-0*, green fluorescence produced by *NLS-ΔspAVR2-GFP* was detected predominantly in the nuclei of transformed epidermal leaf cells (Figure 4D). The green fluorescence originating from *NLS-ΔspAVR2-GFP* expression was always accompanied by the strong red fluorescence from ER-mRFP (Figure 4D, red fluorescence channel). The finding that the ER-mRFP signal is restricted to the ER of transformed cells validates the use of this protein as a marker for bombarded cells and implies that the spread of the RFP signal involves translocation of the NLS-2xRFP protein rather than its mRNA to the neighboring cells. In *35S::ΔspAVR2/35S::ΔspSIX5 A. thaliana* leaves, the red fluorescence of ER-mRFP was also readily detected, but green fluorescence originating from the NLS-ΔspAvr2-GFP protein was rarely observed in the nucleus of a transformed cell (Figure 4D). Using ER-mRFP as a marker, the number of transformed cells emitting green fluorescence was quantified in bombarded *Col-0* and *35S::ΔspAVR2/35S::ΔspSIX5 A. thaliana* leaves. A significant ($p < 0.001$) difference in detection of the green NLS-ΔspAvr2-GFP signal in the nuclei of transformed cells was found between the two genetic backgrounds. Whereas 83% ± 5% of the nuclei of transformed cells in *Col-0* emitted both red and green fluorescence, only 13% ± 4% of that in *35S::ΔspAVR2/35S::ΔspSIX5 Arabidopsis* emitted both colors. The much lower amount of nuclei containing detectable amounts of the Avr2-GFP protein in *35S::ΔspAVR2/35S::ΔspSIX5*-expressing *Arabidopsis* could be explained by a rapid flux of this protein through plasmodesmata. Our inability to detect Avr2-GFP in *ΔspSIX5*-expressing *Arabidopsis* by confocal microscopy may have been due to a swift diffusion of the protein from the central bombarded cells to neighboring cells, and consequently resulted in a signal below the detection threshold of our microscopes. Nonetheless, the results provide indirect evidence for effector translocation.

To directly visualize cell-to-cell movement of Avr2, we used a single binary vector carrying genes encoding both a C-terminally tagged Avr2-GFP and an ER-localized mCherry-HDEL for infiltration of *N. benthamiana* leaves. In contrast to the particle bombardment experiments, in which only small numbers of cells are transformed, agro-infiltration allows a range of transformation efficiencies by simply adjusting the concentration of *Agrobacterium tumefaciens* cells in the infiltration solution. Using an OD_{600} of 0.1 or 0.05 results in a mosaic of transformed and non-transformed cells in the infiltrated sector, allowing visualization of translocation of Avr2-GFP from multiple transformed cells to a few neighboring non-transformed cells. As before, the ER-localized mCherry served as a marker for cell transformation because the protein is unable to translocate to neighboring untransformed cells. To increase protein expression, we co-infiltrated an *A. tumefaciens* strain carrying a binary vector encoding the silencing suppressor p19 with each sample. Co-infiltrations of the Avr2-GFP/mCherry-HDEL construct were performed in either the presence or absence of *35S:ΔspSIX5* to monitor translocation of Avr2-GFP. To ensure equal *A. tumefaciens* concentrations in the co-infiltrations, we replaced the *35S:ΔspSIX5* strain with a *35S-GUS* strain in the latter infiltrations. In the absence of Six5, transformed cells showed an ER-localized mCherry signal located at the cell periphery and a green Avr2-GFP signal in the cytoplasm and nucleus (Figure 5A). Furthermore, non-transformed adjacent cells did not fluoresce red or green in the absence of Six5 (Figure 5A). In the presence of Six5, however, non-transformed cells showed nuclear and cytoplasmic green fluorescence, but no red fluorescence (Figure 5A, lower panels). This observation provides direct support for Six5-mediated translocation of Avr2-GFP from transformed cells to adjacent non-transformed cells.

To assess, in an unbiased manner, the Six5-mediated translocation of Avr2-GFP, we isolated protoplasts from *ΔspAvr2-GFP/mCherry-HDEL* agro-infiltrated leaves and counted the number of green/red fluorescent cells using flow cytometry. To establish the autofluorescence background, we used untransformed cells as a reference; a representative mock is shown in Figure 5B. Based on the mock, four quadrants could be established following expression of the *ΔspAvr2-GFP/mCherry-HDEL* construct. These quadrants represent: Q1, non-transformed cells; Q2, mCherry-expressing cells; Q3, mCherry + GFP-expressing cells; and Q4, GFP-only-containing cells (Figure 5B, middle and right panels). Comparison of Q4 in the absence and presence of Six5 showed an increase in the number of GFP-only cells in the presence of Six5 (Figure 5B) from approximately 0.5% of the total GFP population (Q3 and Q4) to approximately 4% (Figure 5C). In three independent biological replicates, each of which consisted of three infiltrated leaves and subsequent cell counts, a 2- to 7-fold increase in the GFP-only population was observed, in the presence of Six5, in comparison to the GUS control. Whether Six5 itself is

Figure 5. Six5-Mediated Intercellular Translocation of Avr2 in *N. benthamiana*.

(A) Co-agro-infiltration of strains carrying a binary vector encompassing genes encoding mCherry-HDEL and Avr2-GFP with either a *35S:ΔspSIX5* or *35S:GUS*-containing strain into *N. benthamiana* leaves. Fluorescence was analyzed 72 h after infiltration using confocal microscopy. Transformed cells show both a red ER-localized signal and a green Avr2-GFP signal localized to cytoplasm and nucleus (indicated by an asterisk). The ER-localized mCherry is unable to move to neighboring untransformed cells and serves as a marker for transformation. In the absence of Six5, no red or green fluorescence was observed in untransformed cells adjacent to transformed cells (top panels). In the presence of Six5, untransformed cells that flank a transformed cell show green fluorescence in cytoplasm and occasionally in the nucleus, indicating cell-to-cell translocation of Avr2-GFP (indicated by arrows).

(B) To assess Six5-mediated translocation of Avr2-GFP, protoplasts were isolated from *ΔspAvr2-GFP/mCherry-HDEL* agro-infiltrated leaves and the number of cells showing only green, only red, or both green and red fluorescence was counted using flow cytometry. Background autofluorescence levels were determined using untransformed cells (mock) as reference. Based on the mock, four quadrants were established following expression of the *ΔspAvr2-GFP/mCherry-HDEL* construct: Q1, non-transformed cells; Q2, cells expressing mCherry only; Q3, cells expressing mCherry + GFP; and Q4, accumulating GFP only. In the presence of Six5, a higher number of GFP-only cells was observed in Q4 as compared to that of the GUS infiltrations.

(C) In the absence of Six5, approximately 0.5% of the total GFP population (Q3 + Q4) represents GFP-only cells whereas in the presence of Six5 a greater proportion was observed at approximately 3.8%. Three independent biological replicates were performed, one typical example of which is shown here, consisting of three infiltrated leaves and a subsequent count of 50 000 cells per leaf sample.

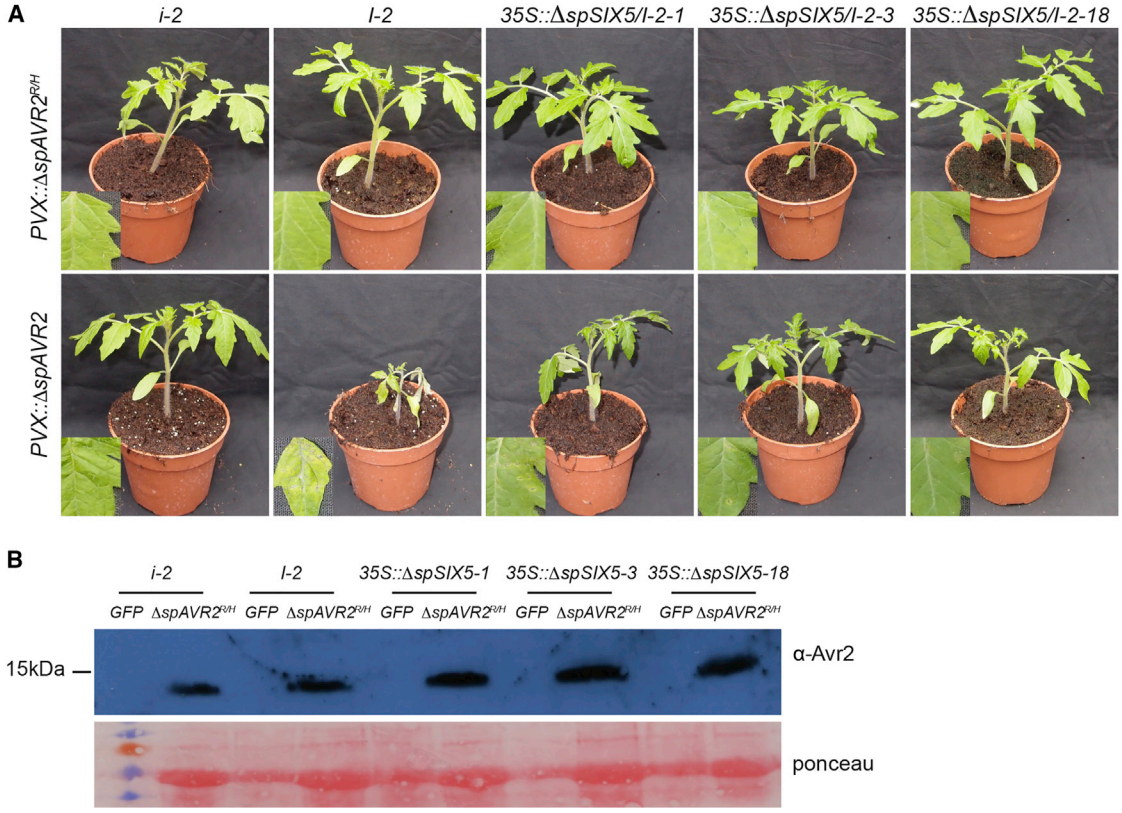

Figure 6. The Avr2/*I-2*-Mediated Hypersensitive Response is Delayed in *SIX5* Transgenic Tomato.
Tomato plants were inoculated with *PVX*::*ΔspAVR2* and *PVX*::*ΔspAVR2*$^{R/H}$ and photographed at 21 dpi.
(A) The upper panel shows *PVX*::*ΔspAVR2*$^{R/H}$-inoculated plants that did not develop an HR. The lower panel shows the systemic HR that developed in *PVX*::*ΔspAVR2*-inoculated *I-2* tomato that showed a severely impaired growth. In *ΔspSIX5/I-2* plants, the HR was delayed and plants were only mildly stunted in comparison with the inoculated *i-2* controls.
(B) Immunoblot showing comparable amounts of Avr2$^{R/H}$ in *PVX*::*ΔspAVR2*$^{R/H}$-infected wild-type and *SIX5* tomato plants. Total protein extracts were subjected to immunoblot analysis and probed with an Avr2 antibody. Ponceau staining shows equal protein loading of *PVX*::*GFP*- or *PVX*::*ΔspAVR2*$^{R/H}$-inoculated tomato lines.

also able to translocate remains unknown; experiments using *ΔspSIX5-GFP/mCherry-HDEL* were inconclusive due to the relatively low fluorescence of the Six5-GFP signal, which was about 10 times weaker than that of Avr2-GFP (Supplemental Figure 3). Based on these data, we conclude that only in the presence of Six5 is Avr2 translocated from transformed to non-transformed *N. benthamiana* cells.

Initiation and Development of *I-2*-mediated HR Following Systemic Spread of *PVX*::*ΔspAVR2* Is Delayed in *SIX5* Tomato

The single-cell transformation experiments in *Arabidopsis* and *N. benthamiana* show that Avr2 is transported to neighboring plant cells only in the presence of Six5. To assess whether Six5-mediated Avr2 translocation also occurs in tomato, we used its ability to trigger an I-2-mediated immune response as a proxy for translocation (Houterman et al., 2009). For expression of *ΔspAVR2* in *I-2* tomato plants, a potato virus X (PVX)-based expression system was employed. Expression of *ΔspAVR2* by PVX triggers an I-2-dependent HR, which is visible as trailing necrosis around the vasculature when the virus spreads systemically through the plant (Houterman et al., 2009). If Six5 alters the distribution pattern of Avr2, one would expect that the pattern of necrotic cell death following spread of the virus in an *I-2*-containing plant to differ from that of a *ΔspSIX5/I-2* plant. Three independent transgenic *ΔspSIX5/I-2* tomato lines were generated that stably expressed the *ΔspSIX5* gene driven by a CaMV 35S promoter (see Methods). Subsequently, *PVX*::*ΔspAVR2* was toothpick-agro-inoculated (Takken et al., 2000) on *i-2* tomato plants (susceptible line C32), *I-2* plants (resistant line), and the three independent homozygous *ΔspSIX5/I-2* tomato lines. The same genotypes were inoculated with the *PVX*::*ΔspAVR2*$^{R/H}$ construct to allow us to distinguish *ΔspAVR2/I-2*-mediated HR from disease symptoms caused by PVX infection (Houterman et al., 2009). Consistent with the observations made by Houterman et al. (2009), no HR was observed following *PVX*::*ΔspAVR2*$^{R/H}$ inoculation (Figure 6A, upper panel; the lower left corner insets show close-up views of the representative leaf). As expected, susceptible *i-2* tomato plants also did not show an HR or chlorosis upon inoculation with *PVX*::*ΔspAVR2*. However, consistent with expression of *I-2* in the vasculature, in *I-2* tomato plants, systematic HR around the vasculature and at leaf tips was detected nine days post inoculation (dpi). Interestingly, no HR was detectable in inoculated *ΔspSIX5/I-2*

plants at this time point (data not shown). The growth of *PVX*::*ΔspAVR2*-inoculated *SlX5* tomato lines was unaffected and the inoculated plants had sizes similar to those of *PVX*::*ΔspAVR2*$^{R/H}$-inoculated tomato lines. At 21 dpi, however, *PVX*::*ΔspAVR2*-inoculated *ΔspSlX5/I-2* plants became moderately stunted and grew slightly smaller than the susceptible controls (*i-2*) (Figure 6A, lower panel). In *ΔspSlX5/I-2* plants, a few necrotic spots emerged along the main leaf veins and close to the leaf tips in fully expanded leaves (Figure 6A, lower panel; the close-ups are representative leaves exhibiting necrosis). At this time point, massive necrosis had developed in *PVX*::*AVR2*-infected *I-2* plants, and these plants were severely stunted while their leaves became chlorotic. Typically, around four weeks after inoculation, all *PVX*::*AVR2*-infected *I-2* plants were dead. *PVX*::*ΔspAVR2*-infected *ΔspSlX5/I-2* plants, however, continued to grow (plants were monitored until eight weeks after inoculation with *PVX*::*ΔspAVR2*), although necrosis progressed and necrotic sectors eventually developed in all fully developed leaves. Hence, compared with wild-type *I-2* plants, HR onset is severely delayed and less pronounced in *ΔspSlX5/I-2* tomato following inoculation with *PVX*::*ΔspAVR2*.

To test whether the observed differences in onset and pattern of cell death is due to (a) reduced accumulation of Avr2 or (b) altered distribution of Avr2, we performed immunoblot analyses. As cell death prohibited a reliable protein extraction from *PVX*::*ΔspAVR2*-inoculated *I-2* tomato lines (data not shown), the accumulation of Avr2$^{R/H}$ was monitored nine days post-PVX inoculation in the second leaf counted from the top of a plant. The Avr2$^{R/H}$ protein has similar properties and the same subcellular localization as Avr2 (Figure 3). Comparable amounts of Avr2$^{R/H}$ were detected in all five *PVX*::*ΔspAVR2*$^{R/H}$-inoculated tomato lines (Figure 6B), which implies that the compromised HR in *I-2*/*ΔspSlX5* tomato is not due to a reduced accumulation of the Avr2 protein following PVX-mediated expression, but possibly to an altered distribution pattern.

Six5 Changes the Distribution of Avr2 in Tomato

The presence of Six5 compromised HR following *PVX*::*ΔspAVR2* infection of *I-2* tomato plants, but did not affect accumulation of the Avr2$^{R/H}$ protein. To assess whether Six5 alters the localization pattern of Avr2 in PVX-infected leaves of *I-2* and *ΔspSlX5/I-2* tomato, we monitored the presence and distribution of a fluorescently labeled Avr2-GFP protein upon inoculation with a recombinant *PVX*::*ΔspAVR2-GFP* construct. Since *PVX*::*ΔspAVR2-GFP* was severely affected in its ability to induce *I-2*-mediated HR in tomato (data not shown), a trimmed Avr2 variant was used that lacks the first 37 amino acids of the N terminus. This truncated Δ37Avr2 protein elicits a faster and stronger *I-2*-mediated HR in *N. benthamiana* than Avr2 (Ma et al., 2013). *PVX*::*Δ37AVR2-GFP* was introduced into 10-day-old *I-2* and *ΔspSlX5/I-2* tomato seedlings by agro-mediated toothpick inoculation. Necrosis developed three weeks after inoculation with *PVX*::*Δ37AVR2-GFP* and, as before, HR development in *ΔspSlX5/I-2* tomato was delayed and reduced as compared to that of *I-2* tomato. Small necrotic spots were observed adjacent to the leaf main veins in fully expanded leaves and occasionally in the tips of newly developing leaves of the Six5-containing plants. In contrast, strong chlorosis and extensive necrosis was found along the major veins of all leaves of the *I-2* wild-type tomato, thereby exhibiting the functionality of the PVX-encoded GFP-tagged Δ37Avr2 protein (data not shown).

To monitor the distribution of the GFP signal, we harvested the second fully expanded leaf (counting from the top) of an inoculated *I-2* or Δsp*SlX5/I-2* tomato plant and subjected it to confocal microscopy analysis. Leaves were harvested at 21 dpi before a visible HR developed, and green fluorescence originating from the Δ37AVR2-GFP protein was observed mostly in the nuclei from both *I-2* and Δsp*SlX5/I-2* tomato leaves (Figure 7A). Numbers of green fluorescent cells observed in *ΔspSlX5*-expressing tomato were greater than in wild-type *I-2* tomato (Figure 7A). As shown in the merged green fluorescence/bright-field images, there are distinct differences in the distribution of the green fluorescence between *I-2* and *ΔspSlX5/I-2* tomato plants (Figure 7A). In *I-2* plants, the Δ37Avr2-GFP signal was mostly localized in cells that are in close vicinity of the leaf vessels, whereas in *ΔspSlX5/I-2* leaves, more cells emitting green fluorescence were observed, and these fluorescent cells were also found at further distances from the veins. To quantify the number of cells along the leaf veins that expressed Δ37Avr2-GFP in *I-2* and *ΔspSlX5/I-2* tomato leaves, we used an ImageJ script to count the number of green nuclei per frame (Jiang et al., 2015). Analyzing 15 frames/genotype revealed an average number of green fluorescent cells in *I-2* tomato plants of 35.1 ± 9.46 per frame while in *ΔspSlX5/I-2* tomato, this number was about three times higher (96.3 ± 20.87, Figure 7B). This significant difference ($p < 0.001$) shows that expression of *ΔspSlX5* altering the distribution of ΔspAvr2 can also occur in tomato.

DISCUSSION

Avr2 and Six5 are both required for fungal virulence and to trigger *I-2*-mediated resistance in tomato (Ma et al., 2015). Here we show that Avr2 and Six5 interact at plasmodesmata. Their combined presence in a plant cell alters the physical properties of the plasmodesmata, allowing NLS-2xRFP and Avr2-GFP to move to neighboring cells (Figure 7C). Whereas these effector proteins are restricted to the transformed cells in the absence of Six5, they were found to move to neighboring cells only in the presence of Six5. The observation that NLS-2xRFP was detected in the nuclei of neighboring cells shows that part of the protein pool was transported before it was translocated to the nucleus. When ER-mRFP encoding constructs were co-bombarded with *ΔspAvr2-GFP* into *ΔspSix5*-expressing *Arabidopsis* leaves, or co-expressed in *N. benthamiana*, red fluorescence was observed only in the ER of the transformed cell and not in the neighboring cells. These observations imply a greater likelihood that the protein of NLS-2xRFP, and not its transcript, is translocated in the presence of Six5 and Avr2, as in the latter case, and consequently the ER of neighboring cells would become red fluorescent.

Using three different experimental systems, we provided data in support of Six5-dependent cell-to-cell movement of Avr2 in tomato, *Arabidopsis*, and *N. benthamiana.* The finding that the effector can spread in three evolutionarily distinct plant species implies that the Avr2/Six5 effector pair targets a

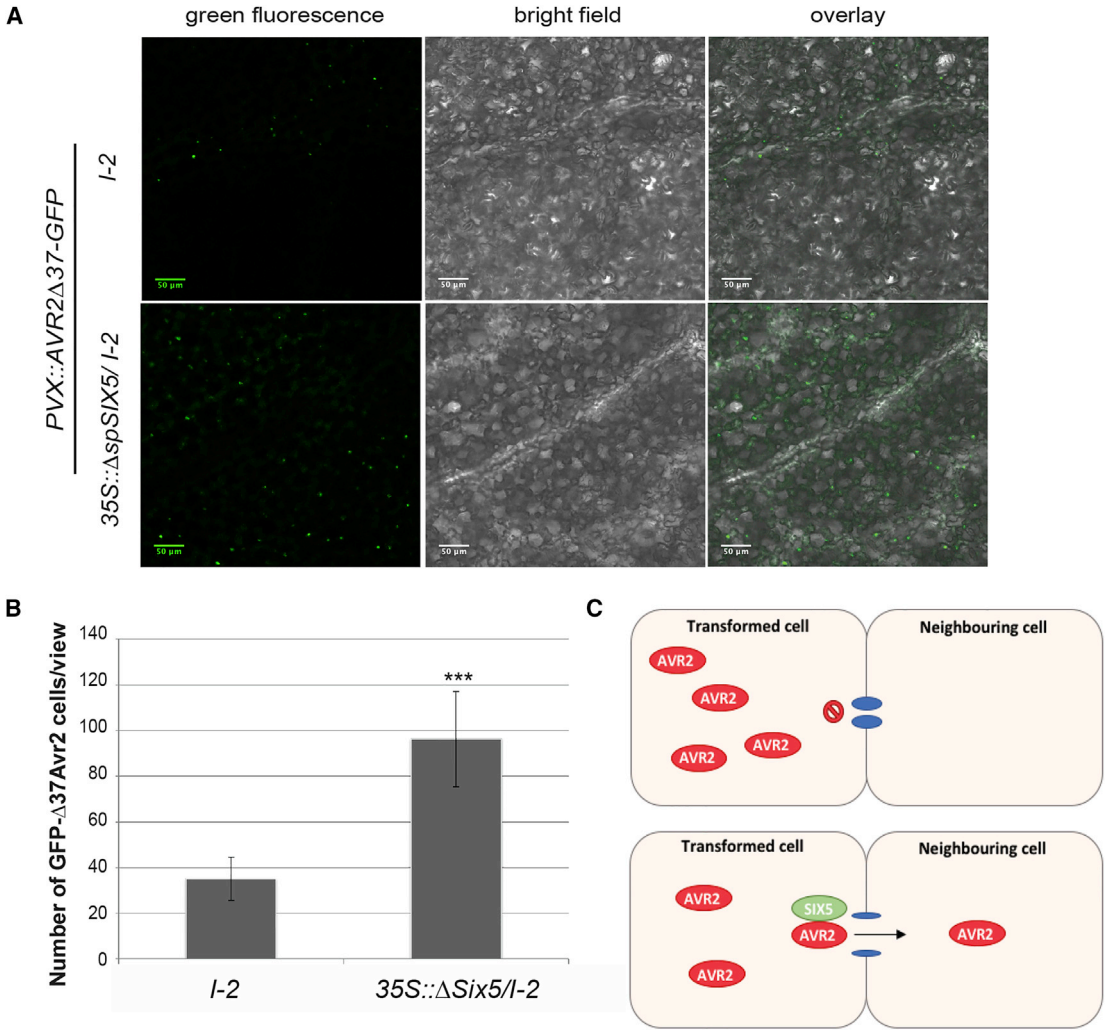

Figure 7. Distribution of Avr2Δ37-GFP Differs between Wild-Type and *35S::ΔspSIX5* Tomato Following *PVX::Avr2Δ37-GFP* Infection.

(A) Representative images of *PVX::Avr2Δ37-GFP*-inoculated *I-2* and *35S::ΔspSIX5/I-2* tomato leaves at 21 dpi. In wild-type *I-2* tomato, the green fluorescence of Avr2Δ37-GFP was mostly localized in cells adjacent to the vessels. In *35S::ΔspSIX5/I-2* tomato leaves, the Avr2Δ37-GFP fluorescence spread to cells further from the vessels and was detected in a larger area.

(B) The number of green fluorescent tomato cells along the leaf vessels containing Avr2Δ37-GFP. Quantification was performed in *I-2* and *35S::ΔspSIX5/I-2* tomato using ImageJ. Fifteen slides were analyzed for each genotype, and an average number of 35.1 ± 9.46 green fluorescent cells per view in *I-2* tomato plants and 96.3 ± 20.87 per view in *SIX5/I-2* tomato were recorded. ***$p < 0.001$.

(C) Graphical model depicting the alteration of the plasmodesmatal size exclusion limit by the *Fusarium oxysporum* Avr2-Six5 effector pair facilitating cell-to-cell movement of Avr2.

conserved process regulating plasmodesmatal SEL. The potential plasmodesmatal protein involved in this process is unknown, and pull-down experiments and extensive Y2H screens have not revealed obvious candidates (Ma et al., 2015). BiFC experiments showed that upon overexpression of Avr2 and Six5, both proteins also interacted in the cytosol. Occasionally, following co-expression of *ΔspSIX5* and the *ΔspAVR2*$^{R/H}$ variant that typically accumulates to slightly higher levels (Houterman et al., 2009), fluorescence complementation was also observed in the nucleus. At lower expression levels, however, fluorescence complementation was only observed at plasmodesmata, suggesting that a plasmodesmata-localized protein stabilizes their interaction (data not shown). Revealing the identity of this protein targeted by the effector pair remains a subject for future studies.

The onset and severity of the systemic HR in *I-2* and *ΔspSIX5/I-2* tomato following *PVX::AVR2* inoculation was severely delayed in the latter transgenic tomato. Whereas accumulation of Avr2$^{R/H}$ was unaffected, the distribution of the Δ37Avr2-GFP protein in the leaf was altered and fluorescence was observed in more cells that were also found at greater distances from the vasculature. This altered distribution, correlating with a delayed and reduced onset of HR, may have different causes. Possibly, the virus can spread more efficiently due to the presence of Avr2 and Six5. One speculation is that the effector pair functionally mimics a viral movement protein. If so, one would predict an enhanced HR phenotype, which was not observed. Alternatively, the delayed onset of HR can be explained by the assumption that in I-2-containing cells, the concentration of Avr2 should exceed a specific threshold before HR is initiated. PVX systemically spreads

through plants, via the vasculature (Baulcombe et al., 1995), from where it infects the *I-2*-expressing cells localized in this tissue (Mes et al., 1999). In the absence of Six5, Avr2 cannot move to neighboring cells. Thus in *PVX*::*ΔspAVR2*-infected wild-type tomato, the Avr2 protein will accumulate in the *I-2*-expressing cells aligning the vasculature. Containment would enable the elicitor to reach a tentative I-2 activation threshold earlier than in *ΔspSIX5* plants, in which the effector can freely move to neighboring cells. This hypothesis is consistent with the observation that the overall amount of Avr2 protein in PVX-infected leaves was the same for wild-type and *ΔspSIX5* plants. The threshold hypothesis is further supported by the observation that only relatively high amounts of Avr2, e.g., following agro-infiltration in *N. benthamiana* or upon PVX-based expression in *I-2* tomato, result in an HR, whereas an HR is not observed in *I-2* tomato following infection with an avirulent *Fol* strain (Houterman et al., 2009; Ma et al., 2015).

A premise of the hypothesis that Six5 facilitates translocation of Avr2, which in susceptible tomato plants likely benefits *Fol* infection as Avr2 is a potent PTI suppressor (Di et al., 2017), implies an obligatory dependency of the effectors on each other to function. Indeed, *Six5* and *Avr2 Fol* knockout strains are equally impaired in their ability to cause disease (Ma et al., 2015). Furthermore, both knockout strains have a highly similar effect on the xylem sap proteome composition, pointing to a largely overlapping activity *in planta* (Gawehns et al., 2015). Also, the observation that expression of both effector genes is driven by a shared promoter region (Schmidt et al., 2013) and that they always occur as a gene pair in *Fol* (Ma et al., 2015) suggest that they function together. Transient expression of *Avr2* alone is sufficient to trigger *I-2*-mediated signaling in *N. benthamiana*, yet Six5 is required for I-2-mediated resistance in tomato (Ma et al., 2015). Our finding that Six5 facilitates cell-to-cell transport of Avr2 could provide a mechanistic explanation for these observations (Mes et al., 1999). The fungus secretes Avr2 and Six5 when it infects the roots (Houterman et al., 2007, 2009) and colonizes endodermal cells and the apoplastic spaces between root cortical cells before entering the xylem vessels (van der Does et al., 2008). *Avr2* promoter reporter fusions show that *Avr2* is strongly expressed in these invading hyphae (Ma et al., 2013), and it is likely that the root endodermal and cortical cells take up the secreted effectors from the extracellular space in the presence of the fungus (Di et al., 2016, 2017). These cortical cells do not express *I-2*, and hence are unable to recognize Avr2 and mount an immune response. Following Avr2/Six5 uptake, Six5 assists translocation of Avr2, enabling Avr2 to reach the I-2-containing cells adjacent to the vasculature, resulting in the activation of an immune response. Such a mechanism would explain why loss of either Six5 or Avr2 compromises I-2-mediated immunity, while Avr2 alone suffices to trigger I-2-mediated HR when heterologously expressed inside I-2-containing cells.

Viruses specifically manipulate plasmodesmata and viral movement proteins (MPs) enlarge the exclusion size of plasmodesmata, allowing the virus to move from cell to cell (Wolf et al., 1989). There are two main strategies for viral movement through plasmodesmata: tubule-guided and non-tubule-guided movement (Schoelz et al., 2011). In the first case, MP dramatically restructures the plasmodesmata by removing the desmotubule and ER within plasmodesmata to expand the pore size. For the non-tubule-guided MPs, no major restructuring of plasmodesmata occurs but the SEL is increased. Whether Avr2/Six5 use similar or distinct mechanisms to alter the exclusion limit of plasmodesmata is unclear, but the tools described here will facilitate future studies aimed at elucidating this process. Studies using fluorescently labeled effectors from *Magnaporthe oryzae* revealed that the PWL2 and BAS1 proteins are observed in the cytosol of both invaded and uninvaded neighboring cells (Khang et al., 2010). Possibly, symplastic effector translocation from infected cells to uninfected neighbors via plasmodesmata is a generic property of plant pathogens. If so, it will be interesting to investigate whether these effectors also similarly manipulate the plasmodesmata. To our knowledge, no *M. oryzae* effectors have yet been confirmed to interact with the plasmodesmata, although BAS3 is a likely candidate to do so (Mosquera et al., 2009).

An interesting question is whether Six5 is co-translocated with Avr2 to neighboring cells. Unfortunately, our experiments aimed at showing direct translocation of GFP-tagged Six5 were unsuccessful due to the poor accumulation of the effector. In conclusion, Six5 and Avr2 together function as a fungal movement protein allowing translocation of Avr2 to neighboring cells. We speculate that spread of Avr2 through root tissues facilitates the infection process by suppressing immune responses (Di et al., 2017). It will be interesting to investigate whether other plant pathogens have a similar mechanism to allow effectors to spread to neighboring cells.

METHODS

Plant Material

The *Arabidopsis* ecotype Columbia (Col-0) and *Solanum lycopersicum* cv. C32 (susceptible *i-2* tomato) (Kroon and Elgersma, 1993) and OT364 (resistant *I-2* tomato) (Mes et al., 1999) were used for *SIX5* transformation. The *Arabidopsis* plants used in this study were grown in a growth chamber under short-day conditions with 13 h of dark and 11 h of light at a temperature of 22°C. Tomato plants used for PVX inoculation were grown in a climatized greenhouse at 25°C, 65% relative humidity, and a 16-h photoperiod.

Plant Transformation

For *in planta* production of Six5, the entry vector pENTR207::*ΔspSIX5* (Ma et al., 2015) was recombined into binary vector pGWB402 according to the Gateway protocol for LR recombination reaction (Invitrogen). The resulting vector was introduced by electroporation into *Agrobacterium tumefaciens* strain GV3101 (Berres et al., 1992) or EHA105 (Tang et al., 1996) for *Arabidopsis* or tomato transformation, respectively. *A. tumefaciens* transformants were selected on Luria–Bertani mannitol medium (10 g/l tryptone, 5 g/l yeast extract, 2.5 g/l NaCl, 10 g/l mannitol, and 15 g/l Daishin agar) supplemented with 100 mg/l spectinomycin and 25 mg/l rifampicin.

Arabidopsis Col-0 plants were transformed by the floral dipping method. First-generation transformants were selected on half strength Murashige–Skoog (MS) medium containing kanamycin, timentin, and nystatin (40, 100 and 100 mg/l, respectively) and subsequently transferred to soil. In total, nine independent single insertion lines were selected according to segregation analysis on selective plates, and among these lines were three homozygous T3 lines that were selected and used for particle bombardment assays. Presence of the transgene was confirmed by PCR with primers FP872 (GGG GAC AAG TTT GTA CAA AAA AAG CAG GCT) and FP873 (GGG GAC CAC TTT GTA CAA GAA AGC TGG GT).

S. lycopersicum cv. C32 and OT364 were transformed with pGWB402::*ΔspSIX5* by *Agrobacterium*-mediated transformation (Cortina and Culianez-Macia, 2004). The presence of *SIX5* in transgenic tomato plants was confirmed by PCR with primers FP872 (GGG GAC AAG TTT GTA CAA AAA AAG CAG GCT) and FP873 (GGG GAC CAC TTT GTA CAA GAA AGC TGG GT), and using immunoblots probed with a Six5 antibody (Ma et al., 2015). The ploidy level of *SIX5* transgenic tomato plants was examined by counting the chloroplast numbers in leaf guard cells (Jacobs and Yoder, 1989). Out of 27 regenerated tomato plants, 13 were diploid and contained the *SIX5* transgene. Four independent homozygous single insertion lines were selected according to segregation of the SIX5 gene as confirmed with PCR (primer pair FP872/FP873). Three independent homozygous T3 lines were used in the PVX inoculation assay.

Construction of Double Transformants

35S::*ΔspAVR2* plants were crossed to *35S*::*ΔspSIX5 Arabidopsis*. F3 progeny homozygous for *35S*::*ΔspAVR2*/*35S*::*ΔspSIX5* were obtained by screening on kanamycin plates (40 mg/l kanamycin, 100 mg/l timentin, and 100 mg/l nystatin) and by detection of *AVR2* and *SIX5* using primer pairs: FP2849 (GGA CTG AAT CAC CGC ATT TAC GA)/FP2848 (ACT GAT TGT GGC TGG ACC TC) and FP872/FP873.

Vector Construction

To generate RFP- and GFP-tagged Avr2 and Six5 for subcellular localization studies, we recombined the entry vectors pENTR207::*ΔspAVR2* (Houterman et al., 2009) and pENTR207::*ΔspSIX5* (Ma et al., 2015) into respective binary vectors pGWB454/455 and pGWB451/452 (Nakagawa et al., 2007) according to the Gateway protocol for LR recombination reaction (Invitrogen) to create respectively N- or C-terminal fusions. To construct NLS-2xRFP, we introduced an NLS into the forward primer FP5455 (AAA AGC AGG CTC CAT GCT GCA GCC TAA GAA GAA GAG AAA GGT TGG AGG AGT GAT CAA GGG CGA GG) and amplified the NLS-RFP fragment together with the reverse primer FP5456 (AGA AAG CTG GGT CGC TTG TAC AGC TCG TCC ATG). The fragment obtained with this primer set was used as a template for a second round of PCR with primer set FP872/FP873. The resulting fragment containing the NLS and RFP coding sequences was recombined into binary vector pGWB454 by an LR recombination reaction.

To generate the cell-to-cell movement vector, we used pDONR207::ΔspAVR2 and pDONR207::ΔspSIX5 to amplify the *ΔspAVR2* and *ΔspSIX5* coding sequences with primer sets FP7937 (CAC CAT TTA CGA ACG ATA GCC ATG CCT GTG GAA GAT GCC GAT TC) and FP7938 (ACC ACC CCG GTG AAC AGC TCC TCG CCC TTG CTC ACC ATG GAT CCA TCC TCT GAG ATA GTA AGA TAG TAG), and FP7945 (CAC CAT TTA CGA ACG ATA GCC ATG AGG GAT CAT CAG TAC TGT G) and FP7946 (ACC ACC CCG GTG AAC AGC TCC TCG CCC TTG CTC ACC ATG GAT CCG GCC GCA TCA CAA TAG A), respectively. The obtained fragments were recombined into a linearized cell-to-cell movement vector pZK538 (Feng et al., 2016), and linearization was achieved via inversion PCR using primer set FP7939 (GGC TAT CGT TCG TAA ATG GTG) and FP7940 (GGA TCC ATG GTG AGC AAG GGC GAG GAG CTG TTC ACC GGG GTG GT). Recombination occurred according to the HiFi DNA assembly cloning protocol (NEB).

Protein Extraction and Western Blotting

Tomato leaves were harvested and snap-frozen in liquid nitrogen. After homogenizing with TissueLyser (Qiagen), the plant material was thawed in urea protein extraction buffer (9.5 M urea, 100 mM Tris [pH 6.8], 2% SDS, and 5 mM DTT) and incubated on ice for 15 min (200 μL buffer per 100 mg tissue). Extracts were centrifuged at 12 000 *g* at 4°C for 10 min, and the supernatant was passed through four layers of Miracloth to obtain a total protein extract. Total protein extracts (40 μl) were mixed with Laemmli sample buffer and heated for 1 min at 98°C. The samples were electrophoresed on 14% SDS–PAGE gels and blotted on PVDF membranes by semi-dry blotting. Blocking was performed with 5% skimmed milk powder and hybridization was performed in the presence of 0.1% Tween 20. Primary antibody anti-Avr2 (Ma et al., 2015) was used at a 1:10 000 dilution and the secondary goat-anti-rabbit antibody conjugated with horseradish peroxidase (Pierce, Rockford, IL, USA) was used at a 1:2500 dilution. The presence of Avr2 protein was visualized by ECL using Fujifilm Super RX-N (http://www.fujifilm.com/).

Agro-Mediated Transient Transformation of *N. benthamiana* Leaves and Protoplast Isolation

Agro-infiltration of *N. benthamiana* leaves was performed as described by Ma et al. (2013). For BiFC assays, co-infiltration of *A. tumefaciens* strains containing the *ΔspAVR2* and *ΔspSIX5* BiFC vectors (Ma et al., 2015) and the PDCB1-mCherry encoding construct (Grangeon et al., 2013) were carried out using an OD_{600} of 0.5 for each culture. The leaves were subjected to confocal microscopy 48 h after infiltration. For cell-to-cell movement assays, co-infiltrations of *A. tumefaciens* strains containing *ΔspAvr2-GFP/mCherry-HDEL or ΔspSix5-GFP/mCherry-HDEL* were carried out at an OD_{600} of 0.05 and 0.1, respectively. All other constructs, *35S*::*ΔspAVR2*, *35S*::*ΔspSIX5*, *35S*:*GUS*, and p19, were infiltrated at an OD_{600} of 0.5.

The agro-infiltrated leaves were subjected to confocal microscopy and protoplast isolation 72 h after infiltration. *N. benthamiana* protoplasts were prepared as described by Faraco et al. (2011), with minor modification. Half an agro-infiltrated leaf of 5-week-old plants was cut into 1- to 2-mm leaf strips, submerged in leaf digestion buffer (Faraco et al., 2011), and, without shaking, kept overnight in the dark.

Particle Bombardment

Particle bombardment was performed according to Levy et al. (2007) on 5-week-old wild-type, *35S*::*ΔspSIX5* and *35S*::*ΔspAVR2*/*35S*::*ΔspSIX5* Arabidopsis leaves. Gold particles (Bio-Rad) (1.0 μm) were coated with 25 μg of each plasmid. Fully expanded leaves placed bottom-up on MS plates, were bombarded twice using a Bio-Rad PDS-1000/He Biolistic particle delivery system. Accumulation and location of fluorescent protein was analyzed 12–24 h after bombardment by confocal microscopy.

Confocal Microscopy

Confocal microscopy was performed with an LSM510 (Zeiss, Germany). GFP and BiFC recombination were excited at 488 nm with an Ar-ion laser and emission was recorded at 505–530/550 nm. Excitation of RFP and mCherry was carried out at 543 nm with an HeNe laser and emission was captured with a 565/585–615 nm filter. To visualize callose, we infiltrated 0.1% aniline blue using a needleless syringe into *N. benthamiana* leaves at 0.5 h before analysis. The aniline blue fluorochrome was excited at 405 nm and emission was recorded at 385–470 nm. Multi-labeling with GFP and RFP or BiFC, mCherry, and aniline blue were imaged by sequential scanning to monitor co-localization.

PVX-Based Systemic Expression in Tomato Plants

A. tumefaciens strain GV3101 containing the helper plasmid pSOUP and binary constructs PVX::*ΔspAVR2*, PVX::*ΔspAVR2*$^{R/H}$, or PVX::*Avr2Δ37-GFP* (Houterman et al., 2009) were used. Toothpick inoculation on tomato plants was performed as described previously (Takken et al., 2000). Ten-day-old tomato plants were used for inoculation.

Flow Cytometry

Flow-cytometry analysis was performed on *N. benthamiana* protoplasts, using a BD FACSAria III (BD Biosciences, USA). Protoplasts were identified by size and complexity (forward scatter-A versus side scatter-A). A Neutral Density filter 2.0 was used to keep the forward scatter protoplast on scale. Excitation of GFP was produced at 488 nm and emission was captured at 530/30 nm. mCherry was excited at 561 nm and emission was captured at 610/20 nm. All samples were filtered over a 50-μm mesh prior to analysis. A total of 50 000 cells was analyzed for each

sample. Data were analyzed with Kaluza Flow Cytometry Analysis software version 1.2 (Beckman Coulter, USA).

SUPPLEMENTAL INFORMATION

Supplemental Information is available at *Molecular Plant Online*.

FUNDING

L.C. was financially supported by the China Scholarship Council (File number: 20120220097) program. F.L.W.T. received funding from the European Union's Horizon 2020 research and innovation program under the Marie Skodowska-Curie grant agreement no. 676480 (Bestpass). F.L.W.T., M.C.B., and N.T. were supported by the NWO-Earth and Life Sciences funded VICI project no. 865.14.003.

AUTHOR CONTRIBUTIONS

L.C. and M.C.B. conducted the experiments, L.C., N.T., M.C.B., B.J.C.C., and F.L.W.T. designed the experiments and wrote the paper.

ACKNOWLEDGEMENTS

We are grateful to Christine Faulkner for providing the ER-RFP construct and for useful discussions and feedback on the manuscript; Jean-François Laliberté for providing PDCB1-mCherry; Xiaorong Tao for the pZK538 vector; Harold Lemereis, Thijs Hendrix, and Ludek Tikovsky for plant care; Miriam Smits for tomato transformation; Eleni Spyropoulou, Francesca Maio, and Ronald Breedijk for help with the confocal microscope; Mariliis Tark-Dame for help with the flow cytometry; Harold van den Burg for insightful discussions; and Manon Richard and Magdalena Mazur for their feedback on the manuscript. No conflict of interest is declared.

Received: June 8, 2017
Revised: February 13, 2018
Accepted: February 13, 2018
Published: February 23, 2018

REFERENCES

Baulcombe, D.C., Chapman, S., and Santa Cruz, S. (1995). Jellyfish green fluorescent protein as a reporter for virus infections. Plant J. **7**:1045–1053.

Berres, R., Otten, L., Tinland, B., Malgarini-Clog, E., and Walter, B. (1992). Transformation of vitis tissue by different strains of *Agrobacterium tumefaciens* containing the T-6b gene. Plant Cell Rep. **11**:192–195.

Cortina, C., and Culianez-Macia, F.A. (2004). Tomato transformation and transgenic plant production. Plant Cell Tissue Organ Cult. **76**:269–275.

Crawford, K.M., and Zambryski, P.C. (2000). Subcelluar localization determines the availability of non-targeted proteins to plasmodesmatal transport. Curr. Biol. **10**:1032–1040.

Di, X., Gomila, J., Ma, L., van den Burg, H.A., and Takken, F.L. (2016). Uptake of the *Fusarium* effector Avr2 by tomato is not a cell autonomous event. Front. Plant Sci. **7**:1915.

Di, X., Cao, L., Hughes, R.K., Tintor, N., Banfield, M.J., and Takken, F.L.W. (2017). Structure-function analysis of the Fusarium oxysporum Avr2 effector allows uncoupling of its immune-suppressing activity from recognition. New Phytol. **216**:897–914.

Faraco, M., Di Sansebastiano, G.P., Spelt, K., Koes, R.E., and Quattrocchio, F.M. (2011). One protoplast is not the other!. Plant Physiol. **156**:474–478.

Feng, Z., Xue, F., Xu, M., Chen, X., Zhao, W., Garcia-Murria, M.J., Mingarro, I., Liu, Y., Huang, Y., Jiang, L., et al. (2016). The ER-membrane transport system is critical for intercellular trafficking of the NSm movement protein and tomato spotted wilt tospovirus. PLoS Pathog. **12**:e1005443.

Gawehns, F., Houterman, P.M., Ichou, F.A., Michielse, C.B., Hijdra, M., Cornelissen, B.J., Rep, M., and Takken, F.L. (2014). The *Fusarium oxysporum* effector Six6 contributes to virulence and suppresses I-2-mediated cell death. Mol. Plant Microbe Interact. **27**:336–348.

Gawehns, F., Ma, L., Bruning, O., Houterman, P.M., Boeren, S., Cornelissen, B.J., Rep, M., and Takken, F.L. (2015). The effector repertoire of *Fusarium oxysporum* determines the tomato xylem proteome composition following infection. Front. Plant Sci. **6**:967.

Gehl, C., Waadt, R., Kudla, J., Mendel, R.R., and Hänsch, R. (2009). New GATEWAY vectors for high throughput analyses of protein-protein interactions by bimolecular fluorescence complementation. Mol. Plant **2**:1051–1058.

Grangeon, R., Jiang, J., Wan, J., Agbeci, M., Zheng, H., and Laliberté, J.F. (2013). $6K_2$-induced vesicles can move cell to cell during turnip mosaic virus infection. Front. Microbiol. **4**:351.

Houterman, P.M., Speijer, D., Dekker, H.L., DE Koster, C.G., Cornelissen, B.J., and Rep, M. (2007). The mixed xylem sap proteome of *Fusarium oxysporum*-infected tomato plants. Mol. Plant Pathol. **8**:215–221.

Houterman, P.M., Ma, L., van Ooijen, G., de Vroomen, M.J., Cornelissen, B.J., Takken, F.L., and Rep, M. (2009). The effector protein Avr2 of the xylem-colonizing fungus *Fusarium oxysporum* activates the tomato resistance protein I-2 intracellularly. Plant J. **58**:970–978.

Jacobs, J.P., and Yoder, J.I. (1989). Ploidy levels in transgenic tomato plants determined by chloroplast number. Plant Cell Rep. **7**:662–664.

Jiang, L., Chen, S.H., Chu, C.H., Wang, S.J., Oyarzabal, E., Wilson, B., Sanders, V., Xie, K., Wang, Q., and Hong, J.S. (2015). A novel role of microglial NADPH oxidase in mediating extra-synaptic function of norepinephrine in regulating brain immune homeostasis. Glia **63**:1057–1072.

Jones, J.D.G., and Dangl, J.L. (2006). The plant immune system. Nature **444**:323–329.

Khang, C.H., Berruyer, R., Giraldo, M.C., Kankanala, P., Park, S.Y., Czymmek, K., Kang, S., and Valent, B. (2010). Translocation of *Magnaporthe oryzae* effectors into rice cells and their subsequent cell-to-cell movement. Plant Cell **22**:1388–1403.

Kroon, B.A.M., and Elgersma, D.M. (1993). Interactions between race-2 of *Fusarium oxysporum* f. sp. *lycopersici* and near-isogenic resistant and susceptible lines of intact plants or callus of tomato. J Phytopathol **137**:1–9.

Levy, A., Erlanger, M., Rosenthal, M., and Epel, B.L. (2007). A plasmodesmata-associated β-1,3-glucanase in *Arabidopsis*. Plant J. **49**:669–682.

Ma, L., Cornelissen, B.J., and Takken, F.L. (2013). A nuclear localization for Avr2 from *Fusarium oxysporum* is required to activate the tomato resistance protein I-2. Front. Plant Sci. **4**:94.

Ma, L., Houterman, P.M., Gawehns, F., Cao, L., Sillo, F., Richter, H., Clavijo-Ortiz, M.J., Schmidt, S.M., Boeren, S., Vervoort, J., et al. (2015). The *AVR2-SIX5* gene pair is required to activate *I-2*-mediated immunity in tomato. New Phytol. **208**:507–518.

Mes, J.J., Weststeijn, E.A., Herlaar, F., Lambalk, J.J., Wijbrandi, J., Haring, M.A., and Cornelissen, B.J. (1999). Biological and molecular characterization of *Fusarium oxysporum* f. sp. *lycopersici* divides race 1 isolates into separate virulence groups. Phytopathology **89**:156–160.

Mes, J.J., van Doorn, A.A., Wijbrandi, J., Simons, G., Cornelissen, B.J., and Haring, M.A. (2000). Expression of the *Fusarium resistance* gene *I-2* colocalizes with the site of fungal containment. Plant J. **23**:183–193.

Michielse, C.B., and Rep, M. (2009). Pathogen profile update: *Fusarium oxysporum*. Mol. Plant Pathol. **10**:311–324.

Mosquera, G., Giraldo, M.C., Khang, C.H., Coughlan, S., and Valent, B. (2009). Interaction transcriptome analysis identifies *Magnaporthe oryzae* BAS1-4 as Biotrophy-associated secreted proteins in rice blast disease. Plant Cell **21**:1273–1290.

Nakagawa, T., Suzuki, T., Murata, S., Nakamura, S., Hino, T., Maeo, K., Tabata, R., Kawai, T., Tanaka, K., Niwa, Y., et al. (2007). Improved Gateway binary vectors: high-performance vectors for creation of fusion constructs in transgenic analysis of plants. Biosci. Biotechnol. Biochem. **71**:2095–2100.

Rep, M., van der Does, H.C., Meijer, M., van Wijk, R., Houterman, P.M., Dekker, H.L., de Koster, C.G., and Cornelissen, B.J. (2004). A small, cysteine-rich protein secreted by *Fusarium oxysporum* during colonization of xylem vessels is required for *I-3*-mediated resistance in tomato. Mol. Microbiol. **53**:1373–1383.

Schmidt, S.M., Houterman, P.M., Schreiver, I., Ma, L., Amyotte, S., Chellappan, B., Boeren, S., Takken, F.L., and Rep, M. (2013). MITEs in the promoters of effector genes allow prediction of novel virulence genes in *Fusarium oxysporum*. BMC Genomics **14**:119.

Schoelz, J.E., Harries, P.A., and Nelson, R.S. (2011). Intracellular transport of plant viruses: finding the door out of the cell. Mol. Plant **4**:813–831.

Simons, G., Groenendijk, J., Wijbrandi, J., Reijans, M., Groenen, J., Diergaarde, P., Van der Lee, T., Bleeker, M., Onstenk, J., De Both, M., et al. (1998). Dissection of the fusarium *I2* gene cluster in tomato reveals six homologs and one active gene copy. Plant Cell **10**:1055–1068.

Takken, F., and Rep, M. (2010). The arms race between tomato and *Fusarium oxysporum*. Mol. Plant Pathol. **11**:309–314.

Takken, F.L., Luderer, R., Gabriëls, S.H., Westerink, N., Lu, R., de Wit, P.J., and Joosten, M.H. (2000). A functional cloning strategy, based on a binary PVX-expression vector, to isolate HR-inducing cDNAs of plant pathogens. Plant J. **24**:275–283.

Tang, X., Frederick, R.D., Zhou, J., Halterman, D.A., Jia, Y., and Martin, G.B. (1996). Initiation of the plant disease resistance by physical interaction of AvrPto and Pto kinase. Science **274**:2060–2063.

van der Does, H.C., Duyvesteijn, R.G.E., Goltstein, P.M., van Schie, C.C.N., Manders, E.M.M., Cornelissen, B.J.C., and Rep, M. (2008). Expression of effector gene *SIX1* of *Fusarium oxysporum* requires living plant cells. Fungal Genet. Biol. **45**:1257–1264.

Wolf, S., Deom, C.M., Beachy, R.N., and Lucas, W.J. (1989). Movement protein of tobacco mosaic virus modifies plasmodesmatal size exclusion limit. Science **246**:377–379.